UC Riverside
UC Riverside Previously Published Works

Title

Quantitative Proteomic Analysis Revealed Broad Roles of N6-Methyladenosine in Heat Shock Response.

Permalink

https://escholarship.org/uc/item/16r791h3

Journal

Journal of Proteome Research, 20(7)

Authors

Miao, Weili
Yang, Yen-Yu
Wang, Yinsheng

Publication Date

2021-07-02

DOI

10.1021/acs.jproteome.1c00191

Peer reviewed

Quantitative Proteomic Analysis Revealed Broad Roles of *N*[6]-Methyladenosine in Heat Shock Response

Weili Miao[†],

Department of Chemistry, University of California, Riverside, California 92521-0403, United States

Yen-Yu Yang[†],

Department of Chemistry, University of California, Riverside, California 92521-0403, United States

Yinsheng Wang

Department of Chemistry, University of California, Riverside, California 92521-0403, United States

Abstract

As optimum temperature is essential for all living organisms, heat shock represents a challenging problem for their survival. Therefore, cellular response to heat shock is among the most extensively investigated stress response pathways; however, how the human proteome responds to heat shock has not been comprehensively investigated. In this study, we employed stable isotope labeling by amino acids in cell culture (SILAC), together with liquid chromatography-tandem mass spectrometry (LC-MS/MS) analysis, to fulfill an in-depth analysis of the alterations in the human proteome in M14 human melanoma cells in response to heat shock stress. We found that, after heat shock, 284 and 278 out of the 4319 quantified proteins were with substantially diminished and elevated expressions, respectively. We also examined the alterations in human kinome after heat shock by using our recently developed targeted proteomic method relying on

Corresponding Author: Yinsheng Wang – Department of Chemistry, University of California, Riverside, California 92521-0403, United States; yinsheng.wang@ucr.edu.
[†]W.M. and Y.-Y.Y. contributed equally.

parallel-reaction monitoring. Our results showed that the expression levels of 11 and 22 kinase proteins were increased and decreased, respectively, by at least 1.5-fold upon heat shock. By interrogating publicly available RNA-seq and m^{6}A sequencing data, we observed that the elevated expression of more than 30 proteins, including CHEK1 and CCND3 kinases, could occur via an m^{6}A-mediated mechanism. Furthermore, our results from single-base elongation and ligation-based quantitative polymerase chain reaction (qPCR) amplification (SELECT) and luciferase reporter assays revealed that heat shock gave rise to elevated m^{6}A levels at A280 and A286 sites in the 5′-untranslated region of *HSPH1* mRNA, thereby leading to increased translation of HSPH1 protein. Together, our discovery and targeted proteomic methods revealed the reprogramming of human proteome and kinome upon heat shock stress and provided insights into cellular responses toward heat shock stress.

Graphical Abstract
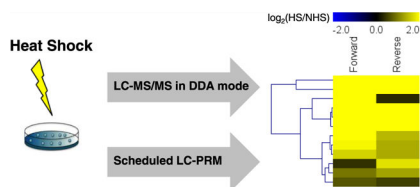
Keywords

quantitative proteomics; parallel-reaction monitoring; heat shock; heat shock proteins; kinase; kinome; N^6-methyladenosine; epitranscriptomics

INTRODUCTION

Organisms have adapted to temperatures of growth in the range of 0–113 °C;[1] nevertheless, heat, as a major form of stress, constitutes a significant life barrier. Temperatures at only moderately above those optimum for growth could confer a survival challenge for living organisms. During heat stress, proteins can also undergo structural alterations, denaturation, and aggregation.[2] Due to the essential role of proteome homeostasis (a.k.a. proteostasis) to cell fitness,[3] heat shock alters critical cellular processes and may lead to cell damage or death.[4] Therefore, cells mount heat shock response to combat the stress.

In response to heat shock, the expression levels of a number of molecular chaperones are elevated to maintain proteostasis, thereby alleviating the impact of increased temperature on proper protein folding.[5] As heat shock response is among the most extensively investigated pathways for stress response in cells, it is crucial to understand its molecular mechanisms. Transcriptomic and proteomic analyses showed that approximately 50–200 genes, including those coding for molecular chaperones and kinases, are significantly induced by heat shock in different model organisms.[4,6–10] However, there is so far no large-scale proteomic analysis about the alterations in the human proteome or kinome in response to heat shock stress.

In this study, we conducted a shot-gun proteomic analysis about the changes in the global proteome of cultured human cells upon heat shock. We identified 284 and 278 proteins that were with diminished and augmented expression levels, respectively, in cells under heat shock. We also examined the heat shock-induced reprogramming of the human kinome with a targeted proteomic method.[11] Our discovery and targeted proteomic analyses together revealed comprehensive changes in the human proteome and kinome in response to heat shock stress. Moreover, we observed that the 5′-UTR of *HSPH1* mRNA could modulate its translation efficiency through an m^6A-dependent epitranscriptomic pathway. Together, our work unveiled comprehensively the heat shock-induced alterations of the human proteome and revealed HSPH1 as a new target for m^6A-mediated epitranscriptomic regulation during heat shock response.

MATERIALS AND METHODS

Cell Culture

M14 (The National Cancer Institute), IGR39 (generous gift from Prof. Peter H. Duesberg),[12] and U2OS (ATCC) cells were maintained in Dulbecco's modified Eagle's medium (DMEM) containing penicillin (100 IU/mL) and 10% fetal bovine serum (Invitrogen, Carlsbad, CA). The cells were cultured at 37 °C in a humidified environment containing 5% CO_2. About 20 million cells were harvested, washed three times with ice-cold phosphate-buffered saline (PBS), and lysed through incubation on ice for 30 min with CelLytic M (Sigma-Aldrich) cell lysis reagent containing 1% protease inhibitor cocktail. The ensuing mixtures were centrifuged for half an hour at 9000g and at 4 °C, and the supernatants were collected. For stable isotope labeling by amino acids in cell culture (SILAC) experiments,[13] the cells were cultured in a medium containing $[^{13}C_6, ^{15}N_2]$-lysine and $[^{13}C_6]$-arginine for a minimum of 2 weeks to facilitate complete incorporation of the stable isotope-labeled amino acids. For heat shock treatment, the cells were maintained for 60 min in a 42.0 °C water bath and then recovered for 6.0 h by incubating at 37 °C.

Sample Preparation and Shot-Gun Proteomic Analysis

The protein lysates of cells with or without heat shock stress (HS and NHS) were mixed at a 1:1 ratio (by mass), and 100 μg of the resultant protein mixture was resolved by a 10% sodium dodecyl sulfate-polyacrylamide gel electrophoresis (SDS-PAGE) gel. Following electrophoresis, the gel lanes were cut into nine sections based on apparent molecular weights (<25, 25–37, 37–42, 42–50, 50–62, 62–75, 75–100, 100–150, >150 kDa). The proteins in individual gel sections were reduced with dithiothreitol, alkylated with iodoacetamide, and digested overnight with modified MS-grade trypsin (Thermo Pierce) in 50 mM NH_4HCO_3 (pH 8.5) at 37 °C, where the trypsin/protein substrate ratio was 1:100. Peptides were subsequently extracted from gels with 5% acetic acid in H_2O and then with 2.5% acetic acid in CH_3CN/H_2O (1:1, v/v). The peptide mixture was then dried, desalted with OMIX C18 tips (Agilent Technologies, Santa Clara, CA), and injected for LC-MS/MS analysis on a Q Exactive Plus quadrupole-Orbitrap mass spectrometer coupled with an UltiMate 3000 UPLC system (Thermo Fisher Scientific). The detailed conditions for liquid chromatography-tandem mass spectrometry (LC-MS/MS) are provided in the Supporting Information.

Maxquant, version 1.5.2.8, was used to analyze the shot-gun proteomic data for protein identification and quantification,[14] with detailed parameters being described in the Supporting Information. Gene Ontology (GO) analysis of the quantified proteins was conducted using the DAVID (version 6.7) bioinformatic tool.[15]

Parallel-Reaction Monitoring (PRM) Analysis of the Human Kinome

The proteins in the light/heavy lysate mixtures were digested with trypsin following the filter-aided sample preparation (FASP) protocol,[16] and a Microcon centrifugal filter (molecular weight cutoff: 30 kDa) was used. Approximately 50 μg of cell lysate was washed with 8 M urea to denature proteins, followed by removal of the urea buffer by centrifugation at 10 000 rpm. The denatured proteins were subjected to reduction, alkylation, and tryptic digestion, as described above. The tryptic digestion mixture of approximately 500 ng of proteins was injected for LC-MS/MS analyses on the Q Exactive Plus mass spectrometer operated in the PRM mode. A maximum of five unique peptides with the strongest precursor ion intensities were selected for each kinase in the isolation list for LC-PRM analysis.

PRM Data Processing

Skyline (version 3.5) was used for processing the PRM data,[17] where we applied a mass accuracy of <20 ppm for fragment ions during peptide identification. We manually inspected the selected-ion chromatograms of targeted peptides to make sure that the different fragment ions from the precursor ions of light and heavy forms of the same peptide share the same retention time. In addition, the light- and heavy-labeled forms of the same peptide should exhibit similar distributions in relative abundances of fragment ions as those in the full-scan MS/MS in the library, with dot product (dotp) values being >0.7.[18] The sum of peak areas of all selected transitions was employed for quantification of the light- or heavy-labeled forms of peptides.

Western Blot and Real-Time Quantitative Polymerase Chain Reaction (RT-qPCR)

M14, IGR39, and U2OS cells were cultured in a 6-well plate or a T-25 flask and lysed at 40–50% confluency following the above-described procedures. The detailed procedures and experimental conditions for Western blot and RT-qPCR analysis are given in the Supporting Information.

Single-Base Elongation and Ligation-Based qPCR Amplification (SELECT) Assay

The SELECT assay for monitoring site-specific m[6]A levels in the 5′-UTR of *HSPH1* mRNA was performed as described previously.[19] The detailed procedures are provided in the Supporting Information.

Dual-Luciferase Reporter Assay

The 5′-UTR of *HSPH1* was subcloned into the *Nco*I site of the pGL3-promoter vector (Promega). The A → C mutations in the 5′-UTR of *HSPH1* were introduced using PCR. All of the plasmids were confirmed by Sanger sequencing, and 1.0 μg of the resulting plasmid was transfected together with 20 ng of pRL Renilla control vector (Promega) into M14 cells cultured in 12-well plates using TransIT-X2 (Mirus Bio). The transfected cells were

subjected to a 1 h heat shock treatment at 42 °C followed by a 0 or 6 h recovery. The cells were lysed, and the luciferase activities were monitored with GloMax Multiplus Plate Reader/Luminometer (Promega) according to the vendor's recommendations.

RESULTS AND DISCUSSION

Differential Expression of Proteins in Response to Heat Shock Stress

The main goal of our study was to examine systematically the heat shock-induced changes in protein expression in cells. To this end, we employed SILAC,[20] along with LC-MS/MS, to analyze the tryptic digestion mixtures of proteins in cells with or without heat shock treatment. For the heat shock treatment, M14 human melanoma cells were cultured at 42 °C for 60 min and then recovered at 37 °C for 6 h. The protein lysates from cells with and without heat shock were resolved by SDS-PAGE, and the resulting gel lane was cut into nine slices. The proteins in individual gel slices were separately digested in-gel with trypsin, and the peptide mixtures were then extracted for LC-MS/MS analysis (Figure 1a).

The LC-MS/MS results led to the quantifications of 4319 proteins; among them, 278 and 284 were up- and downregulated by at least 1.5-fold, respectively, upon heat shock treatment, and the quantification results for those proteins were consistent in forward and reverse SILAC experiments (Table S1). Gene ontology (GO) analysis showed that several groups of proteins were significantly up- or downregulated in cells upon heat shock (*p*-value < 0.05; Figure 1b). Of these groups, heat shock proteins (HSPs),[21] cation transmembrane transporters,[22] protein degradation-related,[23] unfolded protein binding,[24] and GTPases[25] are known to be associated with stress response. Importantly, GO analysis also revealed transferase activity as one of the significantly changed protein groups. This group includes NAPRT1, PARP1, SIRT1, and ZC3HAV1, where the functions of these proteins in heat shock response were not previously known. Thus, the LC-MS/MS data not only validated known proteins but also resulted in the discovery of novel proteins, involved in heat shock response.

HSPs are a family of proteins produced in cells under stress conditions, which was first described in heat shock response.[26] HSPs assume important functions in protein folding, cell cycle regulation, and protection of cells under stress conditions.[27] Our LC-MS/MS data unveiled that 14 heat shock proteins, especially those in the HSP70 and HSP40 families, were upregulated upon heat shock treatment (Figure 2a). We also validated the differential expression of DNAJB4, HSPA1 (HSP70), HSPB8, and HSPH1 in M14 cells in response to heat shock stress by using Western blot analysis, and the results are consistent with those obtained from LC-MS/MS analysis (Figures 2b and S1). In particular, our Western blot analysis showed elevated expressions of HSPB8 and HSPH1 proteins at 1, 3, and 6 h following heat shock in M14 and U2OS osteoblastoma cells (Figure S1). We also observed increased expressions of HSPH1 protein in IGR39 cells following heat shock treatment, though the increases were not statistically significant (Figure S1). We, however, did not observe apparent changes in the levels of HSPB8 protein in IGR39 cells at 1, 3, or 6 h following heat shock. In this vein, it is of note that both M14 and IGR39 melanoma cells carry BRAF-V600E mutation; therefore, these results suggest that the heat shock-induced increases in the expression of HSPB8 protein are independent of this oncogenic mutation.

The unfolded/misfolded proteins, which are induced by heat shock stress and not refolded by HSPs, are degraded by the ubiquitin–proteasome pathway.[28,29] Protein ubiquitination cascade is mediated by ubiquitin-activating enzymes (E1s), ubiquitin-conjugating enzymes (E2s), and ubiquitin ligases (E3s). E3 ubiquitin ligases, which bring ubiquitin-bound E2 and substrate into close proximity so as to enable efficient transfer of E2-conjugated ubiquitin to the protein substrate, are responsible for the specific recognition of substrate proteins in the ubiquitination machinery.[30] Some proteins translated under heat shock are ubiquitinated and subsequently degraded by the proteasome.[23] We observed that heat shock led to the upregulations of five E2 and E3 enzymes (i.e., UBE2G1, UBE2S, UBE2C, MARCH5, and RNF13) and four proteins in the E3-ligase complexes (i.e., UBFD1, UBTD1, KCTD5, KCTD10) (Figure 2c).

Kinome Reprogramming in Response to Heat Shock Stress

Kinases are one of the most important enzyme families involved in cell signaling, represent a group of heat-inducible genes in different model organisms, and are required to further initiate stress response pathways.[4] Therefore, it is important to explore how kinase protein expression is altered during heat shock response. The above-described data-dependent acquisition (DDA) data set led to the quantification of the expression levels of 103 kinases (Figure 2d), among which 7 and 5 were down- (YES1, BTK1, LOC651610, EIF2AK2, STK39, PCK2, POLR2A) and upregulated (CDK6, PKN1, TK1, UCK2, CCND3), respectively, upon heat shock. Considering the superior sensitivity and throughput of the PRM-based targeted proteomics over discovery proteomics,[11,31–39] we further employed scheduled LC-PRM, in combination with SILAC,[20] to examine the differential expression of kinases in response to heat shock (Figure 3a).

The results from the PRM-based targeted proteomic method led to the quantification of a much larger number of unique kinases (285 in total, with ~200 being protein kinases) than DDA analysis (Figures 3b,c and 4; Table S2). It is of note that there were 22 kinases quantified by DDA but not by PRM analysis. Among them, 16 kinases were not included in our PRM library, and 6 escaped PRM detection owing to retention time drift out of the 8 min predicted retention time window. The observed retention times for all of the quantified kinase peptides are linearly correlated with their corresponding normalized retention times (iRTs) in the kinome PRM library (Figure 5a). Additionally, the same retention time was observed for all PRM transitions (4–6 transitions), which exhibit dotp values of >0.7 for each kinase peptide employed for the quantification (Figure 5b).[40] In addition, the quantification results obtained from forward and reverse SILAC labeling experiments are consistent for >90% of the quantified kinase peptides (Figure 5c and Table S2).

Among the 285 quantified kinases, 11 and 22 were increased and decreased by at least 1.5-fold in response to heat shock stress, respectively (Figure 5d). While the ratios obtained from PRM and DDA methods exhibited a similar trend (Figure 5e), PRM yielded better reproducibility among different biological replicates than DDA (Figure 5d).

To validate the PRM results and to assess whether the kinase protein expression upon heat shock treatment is cell type-specific or general, we monitored the expression levels of AK4 protein in two melanoma cell lines (M14 and IGR39) and U2OS osteoblastoma cells at

different time points following heat shock (Figure S1). Our results showed that the AK4 protein level was substantially increased at 1, 3, and 6 h following heat shock in all three cell lines. Together, our findings revealed the rapid modulations of expression levels of kinase proteins in response to heat shock stress.

Protein Expression and m[6]A Levels in Heat Shock Response

To further explore whether the elevated expression of the proteins occurs through transcriptional or post-transcriptional regulation, we analyzed the mRNA and m[6]A levels in the mRNA of the 278 upregulated genes in response to heat shock stress. m[6]A level increases at specific sites in response to heat shock and thus enhances the translation of some heat shock proteins, e.g., HSP70[41] and DNAJB4.[42] Moreover, Liu et al.[43] showed recently that an m[6]A-mediated epitranscriptomic mechanism contributes to elevated expression of AK4 protein in tamoxifen-resistant MCF-7 cells, which confers elevated resistance to tamoxifen in these cells. However, it is unclear whether other targets are regulated in a similar way. Here, we compared the perturbations in proteome with the previously published changes in mRNA levels and their m[6]A levels in mouse embryonic fibroblasts induced by heat shock stress (Figure 6a).[41] We found that, among the 94 overlapped targets, the augmented expression of a total of 32 proteins was accompanied by increased m[6]A levels in their mRNAs (Figure 6b and Table S3).

Six of the 32 proteins, including HSPA1, DNAJB4, DNAJB1, DNAJB6, HSPH1, and BAG3, were with chaperone activity (Figure 6b). HSP70 and DNAJB4 exhibit increased m[6]A levels in the 5′-UTR of their mRNAs in response to heat shock, which promote the translation of these mRNAs.[41,42] This result suggests that heat shock may elicit elevated expression of other heat shock proteins through a similar m[6]A-based epitranscriptomic mechanism.

KCTD10 is a component of Cullin 3-Rbx1-KCTD10 E3-ligase complex involved in protein ubiquitination. Our data suggested KCTD10 as a potential target for m[6]A-modulated expression in heat shock response (Figure 6b). Heat shock is known to elicit ubiquitination and subsequent degradation of unfolded/misfolded proteins in cells.[23,44,45] Our results showed that KCTD10-mediated ubiquitin–proteasome pathway could also be modulated by an epitranscriptomic mechanism involving m[6]A.

Among the 11 upregulated kinases identified by LC-PRM, 2 (CHEK1 and CCND3) exhibited elevated m[6]A levels in their mRNA in response to heat shock stress (Figure 6c–f). Heat shock stress is known to induce DNA damage and inhibit various DNA repair pathways,[46] including base excision repair (BER),[47] nucleotide excision repair (NER),[48] and mismatch repair.[49] Cells under heat stress were previously shown to exhibit increased sensitivity to DNA double-strand break (DSB)-inducing agents (e.g., ionizing radiation).[46] As CHEK1 is involved in both BER and NER pathways[50] and is activated in response to DSBs,[51] it is possible that the heat shock-elicited modulation of DNA damage repair is also modulated by m[6]A. On the other hand, heat shock can lead to a transient cell cycle arrest,[52] and CHEK1 and CCND3 are involved in cell cycle regulation.[53,54] This result suggests that the heat shock-elicited cell cycle arrest may also entail an m[6]A-mediated epitranscriptomic mechanism.

Increased HSPH1 Expression Involves an m^{6}A-Based Mechanism

Among those proteins that are with increased expression and correlated with m^{6}A during heat shock response, an increased m^{6}A level at the 5′-UTR of HSPH1 (a.k.a. HSP105) mRNA potentiated by heat shock was documented to promote the translation efficiency of the mRNA in murine cells in a mechanism independent of the m^{7}G cap.[41] The mechanism, however, was not fully characterized. Since HSPH1 is vital in facilitating the disassembles of misfolded proteins, it is important to understand its translational regulation upon heat shock stress.[55]

We hypothesized that an m^{6}A-based epitranscriptomic regulation at specific sites of the 5′-UTR may also be involved in coordinating the rapid upregulation of HSPH1 protein in M14 cells upon heat shock. To explore this possibility, we employed the SELECT assay[19] to monitor the m^{6}A level of all of the seven putative m^{6}A sites (GAC) in the 5′-UTR of *HSPH1* transcript. In the method, we used DNA probes complementary to the up- and downstreams of the GAC site (Table S4) while keeping a single-nucleotide gap at the site of adenosine under investigation. Modification of the adenosine to m^{6}A would hinder the elongation and ligation at the nick, thereby lowering the yields of the RNA template for qPCR analysis. Strikingly, while the template of the negative control adenosine 115 increased in a magnitude similar to that of *HSPH1* transcript upon heat shock stress, the abundances of the templates from all seven GAC sites were significantly lower, suggesting elevated levels of m^{6}A at its consensus motif sites in the 5′-UTR of *HSPH1* mRNA upon heat shock (Figure 7a–c).

Next, we employed luciferase reporter assay to monitor the effects of m^{6}A in the 5′-UTR of *HSPH1* mRNA on translational efficiencies by mutating the adenosines of interest to cytidines. The results showed that such mutations, which prevent the formation of m^{6}A, at adenosines 280 and 286, suppressed translation efficiency at 6 h following heat shock (Figures 7d and S2).

CONCLUSIONS

By employing SILAC together with LC-MS/MS analysis, we investigated the alterations of the global proteome in cultured human cells in response to heat shock stress, and the analysis led to the identifications of 284 and 278 down- and upregulated proteins, respectively. We also applied our recently developed PRM-based targeted proteomic method to examine the differential expression of kinase proteins in response to heat shock, which revealed the up- and downregulations of 11 and 22 kinases, respectively. In combination with previously published RNA-seq and m^{6}A-seq data, we found that the augmented expression of more than 30 proteins, including 2 kinases (CHEK1 and CCND3), could be regulated by m^{6}A. We further confirmed the elevated m^{6}A level at multiple m^{6}A consensus motif sites in the 5′-UTR of *HSPH1* mRNA and revealed the roles of site-specific m^{6}A in regulating translation efficiency upon heat shock stress.

Together, our study represents the application of state-of-the-art quantitative proteomic methods for interrogating a very important stress response pathway, and our work provided a comprehensive list of target proteins for understanding further the biological responses

associated with heat shock stress. Moreover, we revealed a new target (i.e., HSPH1) in human cells that is subjected to m^{6}A-based epitranscriptomic regulation under heat shock stress.

Supplementary Material

Refer to Web version on PubMed Central for supplementary material.

ACKNOWLEDGMENTS

REFERENCES

(1). Stetter KO Hyperthermophiles in the history of life. Philos. Trans. R. Soc. London, Ser. B 2006, 361, 1837–1843. [PubMed: 17008222]

(2). Weijers M; Barneveld PA; Cohen Stuart MA; Visschers RW Heat-induced denaturation and aggregation of ovalbumin at neutral pH described by irreversible first-order kinetics. Protein Sci. 2003, 12, 2693–2703. [PubMed: 14627731]

(3). Balchin D; Hayer-Hartl M; Hartl FU In vivo aspects of protein folding and quality control. Science 2016, 353, No. aac4354. [PubMed: 27365453]

(4). Richter K; Haslbeck M; Buchner J The Heat Shock Response: Life on the Verge of Death. Mol. Cell 2010, 40, 253–266. [PubMed: 20965420]

(5). Morimoto RI Cells in stress: transcriptional activation of heat shock genes. Science 1993, 259, 1409. [PubMed: 8451637]

(6). Gasch AP; Spellman PT; Kao CM; Carmel-Harel O; Eisen MB; Storz G; Botstein D; Brown PO Genomic Expression Programs in the Response of Yeast Cells to Environmental Changes. Mol. Biol. Cell 2000, 11, 4241–4257. [PubMed: 11102521]

(7). Richmond CS; Glasner JD; Mau R; Jin H; Blattner FR Genome-wide expression profiling in Escherichia coli K-12. Nucleic Acids Res. 1999, 27, 3821–3835. [PubMed: 10481021]

(8). GuhaThakurta D; Palomar L; Stormo GD; Tedesco P; Johnson TE; Walker DW; Lithgow G; Kim S; Link CD Identification of a novel cis-regulatory element involved in the heat shock response in Caenorhabditis elegans using microarray gene expression and computational methods. Genome Res. 2002, 12, 701–712. [PubMed: 11997337]

(9). Finka A; Sood V; Quadroni M; Rios PDL; Goloubinoff P Quantitative proteomics of heat-treated human cells show an across-the-board mild depletion of housekeeping proteins to massively accumulate few HSPs. Cell Stress Chaperones 2015, 20, 605–620. [PubMed: 25847399]

(10). Rosen R; Ron EZ Proteome analysis in the study of the bacterial heat-shock response. Mass Spectrom. Rev 2002, 21, 244–265. [PubMed: 12533799]

(11). Miao W; Guo L; Wang Y Imatinib-induced changes in protein expression and ATP-binding affinities of kinases in chronic myelocytic leukemia cells. Anal. Chem 2019, 91, 3209–3214. [PubMed: 30773012]

(12). Bloomfield M; Duesberg P Inherent variability of cancer-specific aneuploidy generates metastases. Mol. Cytogenet 2016, 9, No. 90. [PubMed: 28018487]

(13). Ong S-E; Blagoev B; Kratchmarova I; Kristensen DB; Steen H; Pandey A; Mann M Stable isotope labeling by amino acids in cell culture, SILAC, as a simple and accurate approach to expression proteomics. Mol. Cell. Proteomics 2002, 1, 376–386. [PubMed: 12118079]

(14). Cox J; Mann M MaxQuant enables high peptide identification rates, individualized p.p.b.-range mass accuracies and proteome-wide protein quantification. Nat. Biotechnol 2008, 26, 1367–1372. [PubMed: 19029910]

(15). Huang DW; Sherman BT; Lempicki RA Systematic and integrative analysis of large gene lists using DAVID bioinformatics resources. Nat. Protoc 2009, 4, 44–57. [PubMed: 19131956]

(16). Wi niewski JR; Zougman A; Nagaraj N; Mann M Universal sample preparation method for proteome analysis. Nat. Methods 2009, 6, 359–362. [PubMed: 19377485]

(17). MacLean B; Tomazela DM; Shulman N; Chambers M; Finney GL; Frewen B; Kern R; Tabb DL; Liebler DC; MacCoss MJ Skyline: an open source document editor for creating and analyzing targeted proteomics experiments. Bioinformatics 2010, 26, 966–968. [PubMed: 20147306]

(18). Sherwood CA; Eastham A; Lee LW; Risler J; Vitek O; Martin DB Correlation between y-type ions observed in ion trap and triple quadrupole mass spectrometers. J. Proteome Res 2009, 8, 4243–4251. [PubMed: 19603825]

(19). Xiao Y; Wang Y; Tang Q; Wei L; Zhang X; Jia G An elongation- and ligation-based qPCR amplification method for the radiolabeling-free detection of locus-specific N(6)-methyladenosine modification. Angew. Chem., Int. Ed 2018, 57, 15995–16000.

(20). Ong S-E; Blagoev B; Kratchmarova I; Kristensen DB; Steen H; Pandey A; Mann M Stable isotope labeling by amino acids in cell culture, SILAC, as a simple and accurate approach to expression proteomics. Mol. Cell. Proteomics 2002, 1, 376–386. [PubMed: 12118079]

(21). Jolly C; Morimoto RI Role of the Heat Shock Response and Molecular Chaperones in Oncogenesis and Cell Death. J. Natl. Cancer Inst 2000, 92, 1564–1572. [PubMed: 11018092]

(22). Conde A; Chaves MM; Gerós H Membrane Transport, Sensing and Signaling in Plant Adaptation to Environmental Stress. Plant Cell Physiol. 2011, 52, 1583–1602. [PubMed: 21828102]

(23). Aprile-Garcia F; Tomar P; Hummel B; Khavaran A; Sawarkar R Nascent-protein ubiquitination is required for heat shock–induced gene downregulation in human cells. Nat. Struct. Mol. Biol 2019, 26, 137–146. [PubMed: 30723328]

(24). Heldens L; Hensen SMM; Onnekink C; van Genesen ST; Dirks RP; Lubsen NH An Atypical Unfolded Protein Response in Heat Shocked Cells. PLoS One 2011, 6, No. e23512. [PubMed: 21853144]

(25). Ralhan R; Kaur J; Tamiz Chelvi P; Singh SP; Zeba H Heat stress stimulates high affinity GTPase in cervical carcinoma cells. Int. J. Biochem. Cell Biol 1995, 27, 263–269. [PubMed: 7780830]

(26). Ritossa F A new puffing pattern induced by temperature shock and DNP in drosophila. Experientia 1962, 18, 571–573.

(27). Feder ME; Hofmann GE Heat shock proteins, molecular chaperones, and the stress response: evolutionary and ecological physiology. Annu. Rev. Physiol 1999, 61, 243–282. [PubMed: 10099689]

(28). Mukhopadhyay D; Riezman H Proteasome-Independent Functions of Ubiquitin in Endocytosis and Signaling. Science 2007, 315, 201. [PubMed: 17218518]

(29). Schnell JD; Hicke L Non-traditional Functions of Ubiquitin and Ubiquitin-binding Proteins. J. Biol. Chem 2003, 278, 35857–35860. [PubMed: 12860974]

(30). Glickman MH; Ciechanover A The Ubiquitin-Proteasome Proteolytic Pathway: Destruction for the Sake of Construction. Physiol. Rev 2002, 82, 373–428. [PubMed: 11917093]

(31). Miao W; Li L; Liu X; Qi TF; Guo L; Huang M; Wang Y A targeted quantitative proteomic method revealed a substantial reprogramming of kinome during melanoma metastasis. Sci. Rep 2020, 10, No. 2485. [PubMed: 32051510]

(32). Miao W; Li L; Wang Y High-throughput targeted quantitative analysis of the interaction between HSP90 and kinases. Anal. Chem 2019, 91, 11507–11509. [PubMed: 31476117]

(33). Miao W; Wang Y Targeted quantitative kinome analysis identifies PRPS2 as a promoter for colorectal cancer metastasis. J. Proteome Res 2019, 18, 2279–2286. [PubMed: 30908912]

(34). Miao W; Wang Y Quantitative interrogation of the human kinome perturbed by two BRAF inhibitors. J. Proteome Res 2019, 18, 2624–2631. [PubMed: 30994353]

(35). Miao W; Yuan J; Li L; Wang Y Parallel-reaction monitoring-based proteome-wide profiling of differential kinase protein expression during prostate cancer metastasis in vitro. Anal. Chem 2019, 91, 9893–9900. [PubMed: 31241916]

(36). Liu X; Miao W; Huang M; Li L; Dai X; Wang Y Elevated hexokinase II expression confers acquired resistance to 4-hydroxytamoxifen in breast cancer cells. Mol. Cell. Proteomics 2019, 18, 2273–2284. [PubMed: 31519767]

(37). Miao W; Li L; Wang Y A targeted proteomic approach for heat shock proteins reveals DNAJB4 as a suppressor for melanoma metastasis. Anal. Chem 2018, 90, 6835–6842. [PubMed: 29722524]

(38). Miao W; Li L; Wang Y Identification of helicase proteins as clients for HSP90. Anal. Chem 2018, 90, 11751–11755. [PubMed: 30247883]

(39). Miao W; Bade D; Wang Y Targeted Proteomic Analysis Revealed Kinome Reprogramming during Acquisition of Radio-resistance in Breast Cancer Cells. J. Proteome Res 2021, 2830–2838. [PubMed: 33739118]

(40). de Graaf EL; Altelaar AF; van Breukelen B; Mohammed S; Heck AJ Improving SRM assay development: a global comparison between triple quadrupole, ion trap, and higher energy CID peptide fragmentation spectra. J. Proteome Res 2011, 10, 4334–4341. [PubMed: 21726076]

(41). Zhou J; Wan J; Gao X; Zhang X; Jaffrey SR; Qian S-B Dynamic m6A mRNA methylation directs translational control of heat shock response. Nature 2015, 526, 591–594. [PubMed: 26458103]

(42). Miao W; Li L; Zhao Y; Dai X; Chen X; Wang Y HSP90 inhibitors stimulate DNAJB4 protein expression through a mechanism involving N6-methyladenosine. Nat. Commun 2019, 10, No. 3613. [PubMed: 31399576]

(43). Liu X; Gonzalez G; Dai X; Miao W; Yuan J; Huang M; Bade D; Li L; Sun Y; Wang Y Adenylate Kinase 4 Modulates the Resistance of Breast Cancer Cells to Tamoxifen through an m^{6}A-Based Epitranscriptomic Mechanism. Mol. Ther 2020, 28, 2593–2604. [PubMed: 32956623]

(44). Mathew A; Mathur SK; Morimoto RI Heat shock response and protein degradation: regulation of HSF2 by the ubiquitin-proteasome pathway. Mol. Cell. Biol 1998, 18, 5091–5098. [PubMed: 9710593]

(45). Goldberg AL Protein degradation and protection against misfolded or damaged proteins. Nature 2003, 426, 895–899. [PubMed: 14685250]

(46). Kantidze OL; Velichko AK; Luzhin AV; Razin SV Heat Stress-Induced DNA Damage. Acta Nat. 2016, 8, 75–78.

(47). Batuello CN; Kelley MR; Dynlacht JR Role of Ape1 and base excision repair in the radioresponse and heat-radiosensitization of HeLa Cells. Anticancer Res. 2009, 29, 1319–1325. [PubMed: 19414382]

(48). Muenyi CS; States VA; Masters JH; Fan TW; Helm CW; States JC Sodium arsenite and hyperthermia modulate cisplatin-DNA damage responses and enhance platinum accumulation in murine metastatic ovarian cancer xenograft after hyperthermic intraperitoneal chemotherapy (HIPEC). J. Ovarian Res 2011, 4, No. 9. [PubMed: 21696631]

(49). Nadin SB; Cuello-Carrión FD; Sottile ML; Ciocca DR; Vargas-Roig LM Effects of hyperthermia on Hsp27 (HSPB1), Hsp72 (HSPA1A) and DNA repair proteins hMLH1 and hMSH2 in human colorectal cancer hMLH1-deficient and hMLH1-proficient cell lines. Int. J. Hyperthermia 2012, 28, 191–201. [PubMed: 22515340]

(50). Yan S; Sorrell M; Berman Z Functional interplay between ATM/ATR-mediated DNA damage response and DNA repair pathways in oxidative stress. Cell. Mol. Life Sci 2014, 71, 3951–3967. [PubMed: 24947324]

(51). Smith J; Mun Tho L; Xu N; Gillespie DA The ATM–Chk2 and ATR–Chk1 Pathways in DNA Damage Signaling and Cancer. In Advances in Cancer Research; Vande Woude GF; Klein G, Eds.; Academic Press, 2010; Chapter 3, Vol. 108, pp 73–112. [PubMed: 21034966]

(52). Kühl NM; Rensing L Heat shock effects on cell cycle progression. Cell. Mol. Life Sci 2000, 57, 450–463. [PubMed: 10823246]

(53). Sawai CM; Freund J; Oh P; Ndiaye-Lobry D; Bretz JC; Strikoudis A; Genesca L; Trimarchi T; Kelliher MA; Clark M; Soulier J; Chen-Kiang S; Aifantis I Therapeutic targeting of the cyclin D3:CDK4/6 complex in T cell leukemia. Cancer Cell 2012, 22, 452–465. [PubMed: 23079656]

(54). Yu H Chk1: A Double Agent in Cell Cycle Checkpoints. Dev. Cell 2007, 12, 167–168. [PubMed: 17276330]

(55). Mattoo RUH; Sharma SK; Priya S; Finka A; Goloubinoff P Hsp110 is a bona fide chaperone using ATP to unfold stable misfolded polypeptides and reciprocally collaborate with Hsp70 to solubilize protein aggregates. J. Biol. Chem 2013, 288, 21399–21411. [PubMed: 23737532]
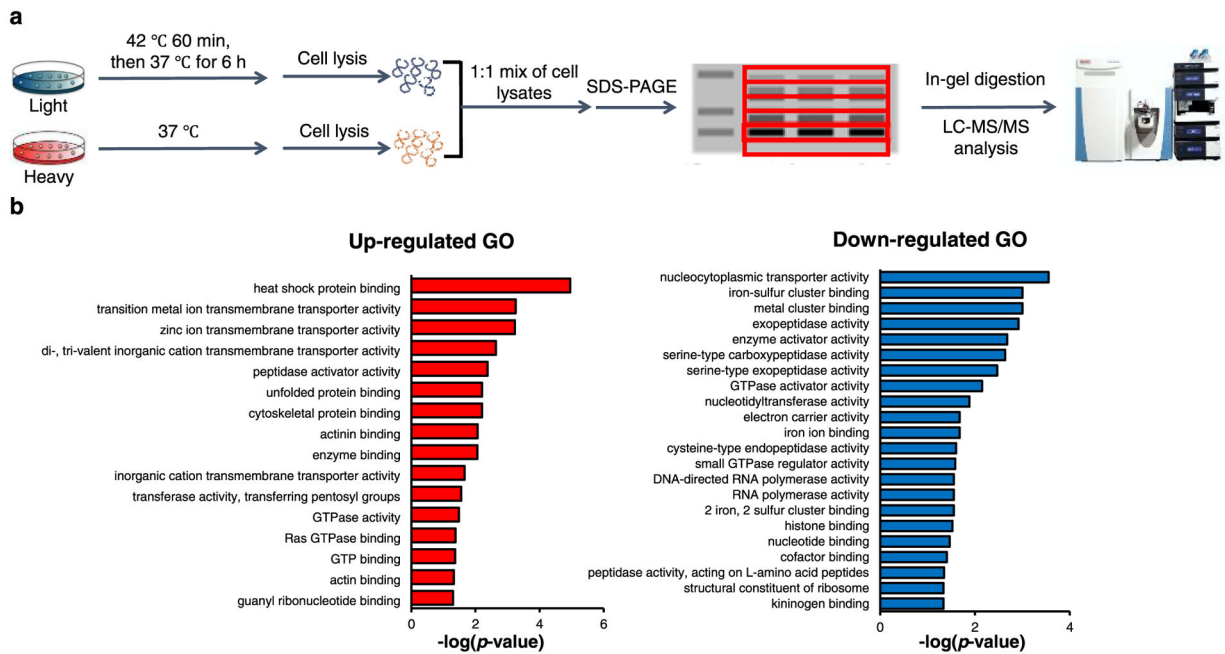
Figure 1.

Discovery proteomic method for exploring differentially expressed proteins in M14 cells in response to heat shock. (a) A diagram depicting the experimental strategy. (b) GO analysis of up- and downregulated proteins in response to heat shock stress. The *p*-value, which was calculated using the DAVID bioinformatic tool, represents the Fisher exact statistics in the DAVID system and refers to a one-tail Fisher exact probability value employed in gene enrichment analysis.
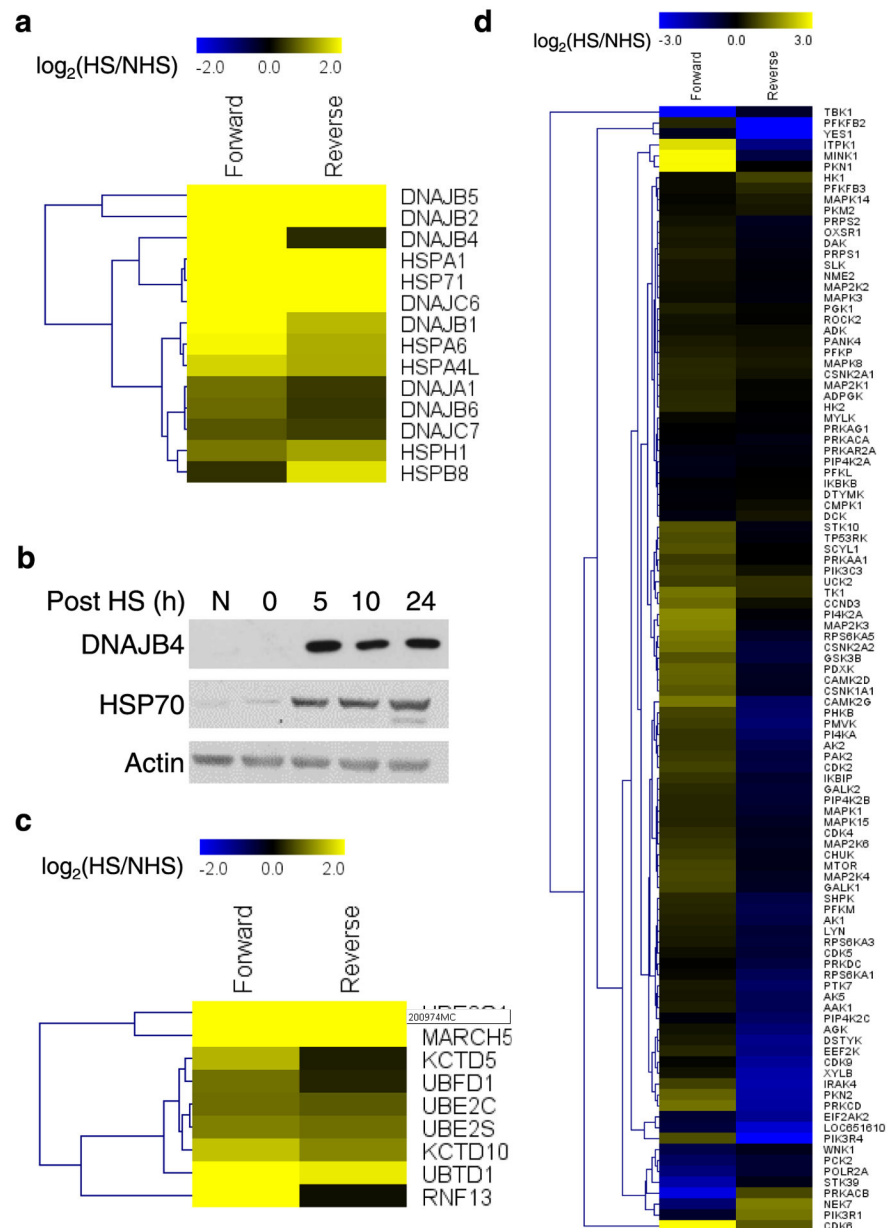
Figure 2.
Perturbations in the human proteome in M14 cells upon heat shock stress. (a) Heat map displaying the perturbations in expression levels of heat shock proteins in response to heat shock (Table S1). (b) Western blot for validating the expression levels of HSP70 and DNAJB4 at different time intervals following heat shock stress. (c) Heat map showing the alterations in protein expression levels of E2 and E3 ubiquitin-modifying enzymes in response to heat shock (Table S1). (d) Heat map showing the perturbations in expression levels of kinases in response to heat shock, as obtained from discovery proteomic analysis (Table S1).
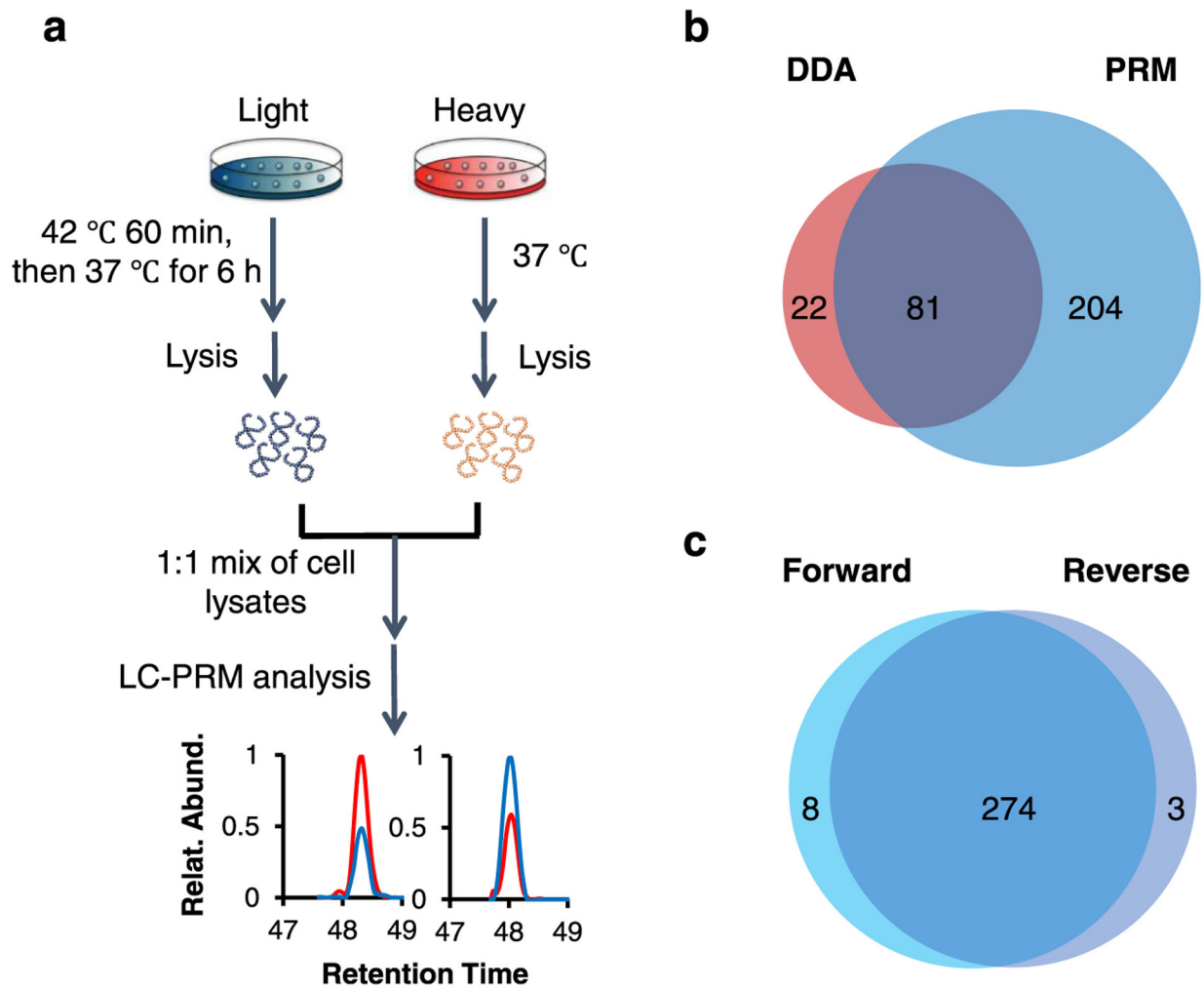
Figure 3.
PRM-based targeted proteomic method revealed changes in protein expression levels of kinases in M14 cells following heat shock. (a) Schematic diagram showing the PRM method. (b) Venn diagram revealing the overlap in the number of kinases that were quantified based on DDA and PRM analyses. (c) Venn diagram showing the overlap in the number of kinases quantified in LC-PRM analysis together with forward and reverse SILAC labelings.
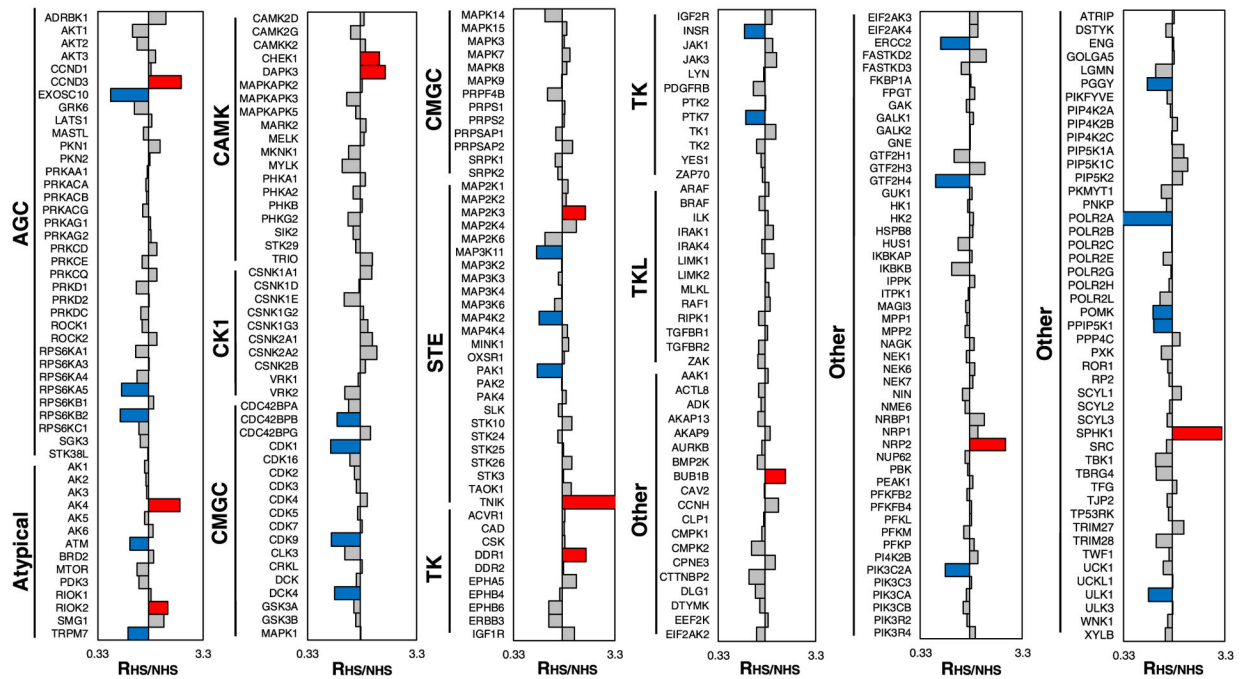
Figure 4.
Differential expression of kinases in M14 cells at 6 h following a 1.0 h heat shock at 42 °C.
Red, blue, and gray bars represent those kinases with ratios (HS/NHS) that are >1.5, <0.67,
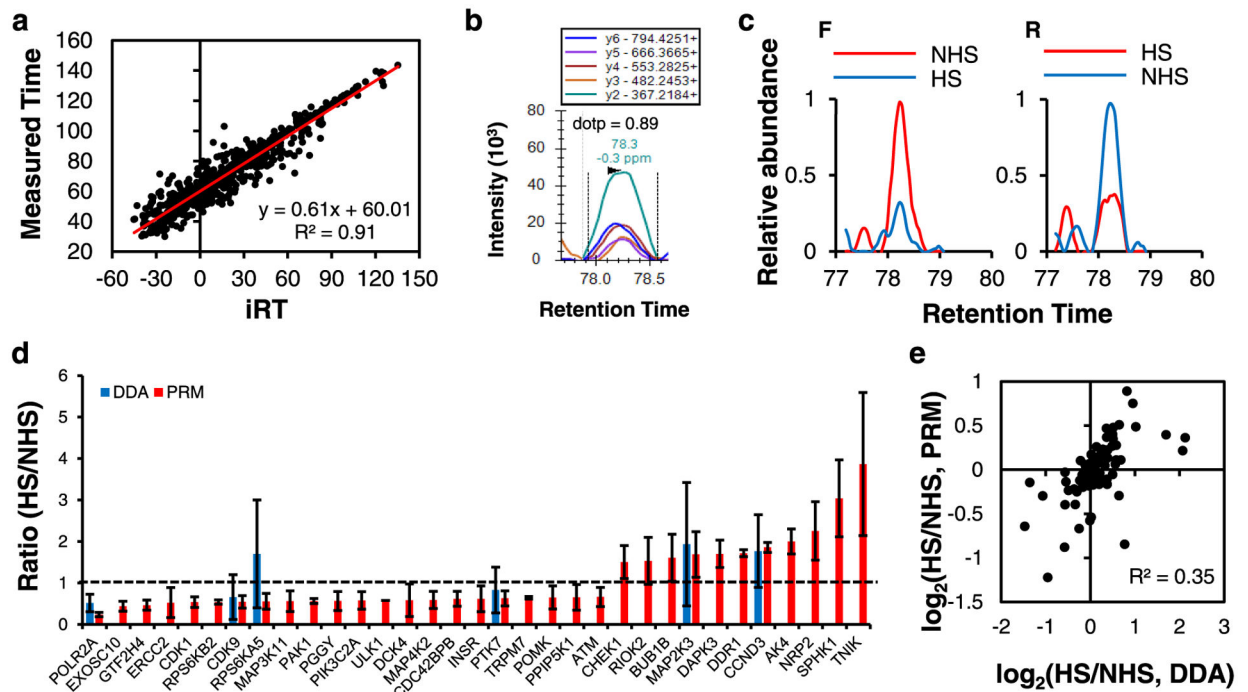and between 0.67 and 1.5, respectively.

Figure 5.
Performances of the LC-PRM analysis. (a) Correlation between iRT in the kinome PRM library and measured RT on a Q Exactive Plus mass spectrometer. (b) Extracted-ion chromatogram for a tryptic peptide, QYQLADWR, from EXOSC10. (c) PRM traces for a tryptic peptide, QYQLADWR, from EXOSC10. (d) Bar graph showing the perturbed kinases in heat shock response. The data represent the mean ± standard deviation (SD) of the quantification results ($n = 2$ for DDA, $n = 3$ for PRM). (e) Scatter plot comparing the ratios of kinases obtained from DDA and PRM analyses.
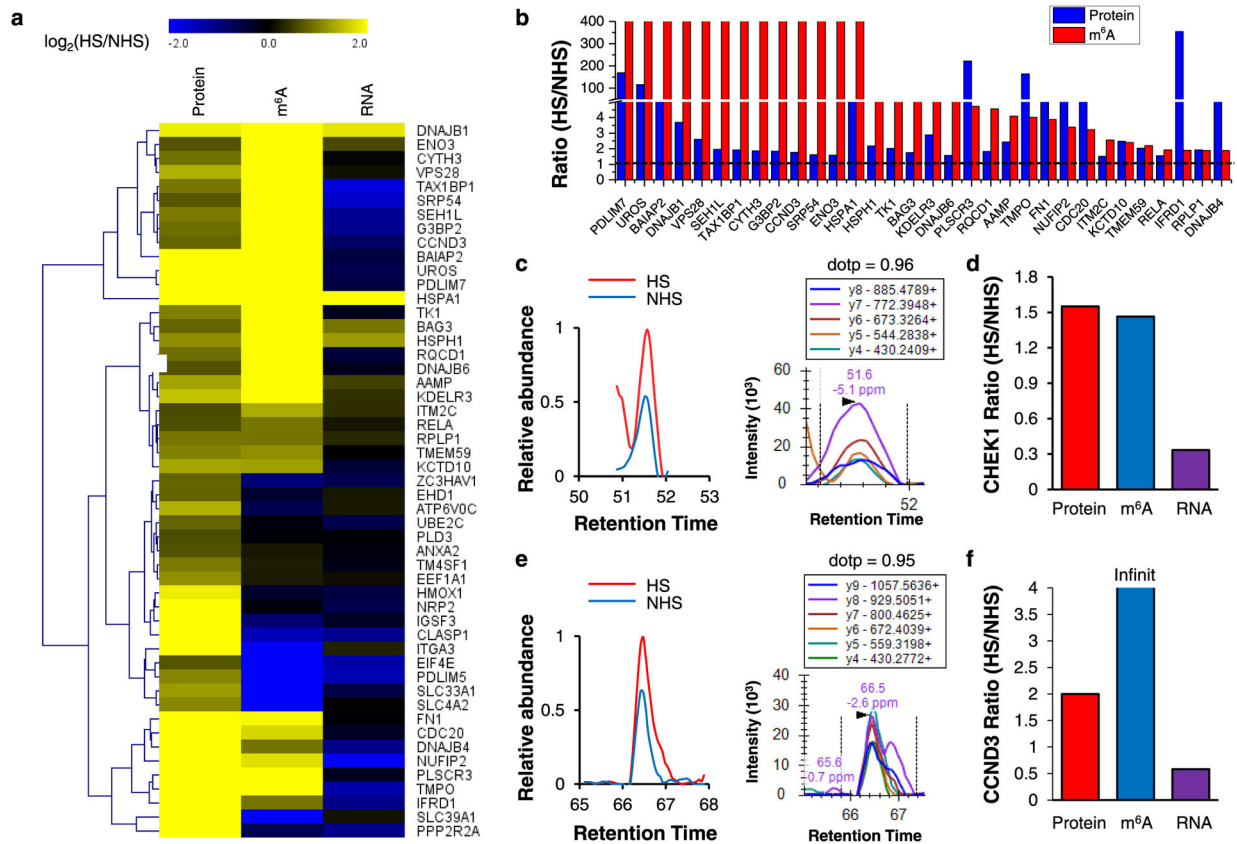
Figure 6.

Protein expression and m6A levels in heat shock response. (a) Comparison of protein, m6A, and mRNA levels of those upregulated proteins in response to heat shock stress. (b) Bar graph showing proteins with elevated expression upon heat shock and the corresponding changes in m6A levels of their mRNAs. (c) PRM traces and extracted-ion chromatograms for representative *y* ions of a tryptic peptide, ILVENPSAR, from CHEK1. (d) Comparison of protein, m6A, and RNA levels of CHEK1 in response to heat shock stress. (e) PRM traces and extracted-ion chromatograms for representative *y* ions for a tryptic peptide, ACQEQIEAALR, from CCND3. (f) Comparison of protein, m6A, and RNA levels of CCND3 in response to heat shock stress. The values represent the fold changes in RPKM reads of m6A and mRNA obtained from publicly available data of m6A-seq and RNA-seq, respectively. 'infinit' indicates a ratio of infinity (i.e., m6A was only detected after heat shock).
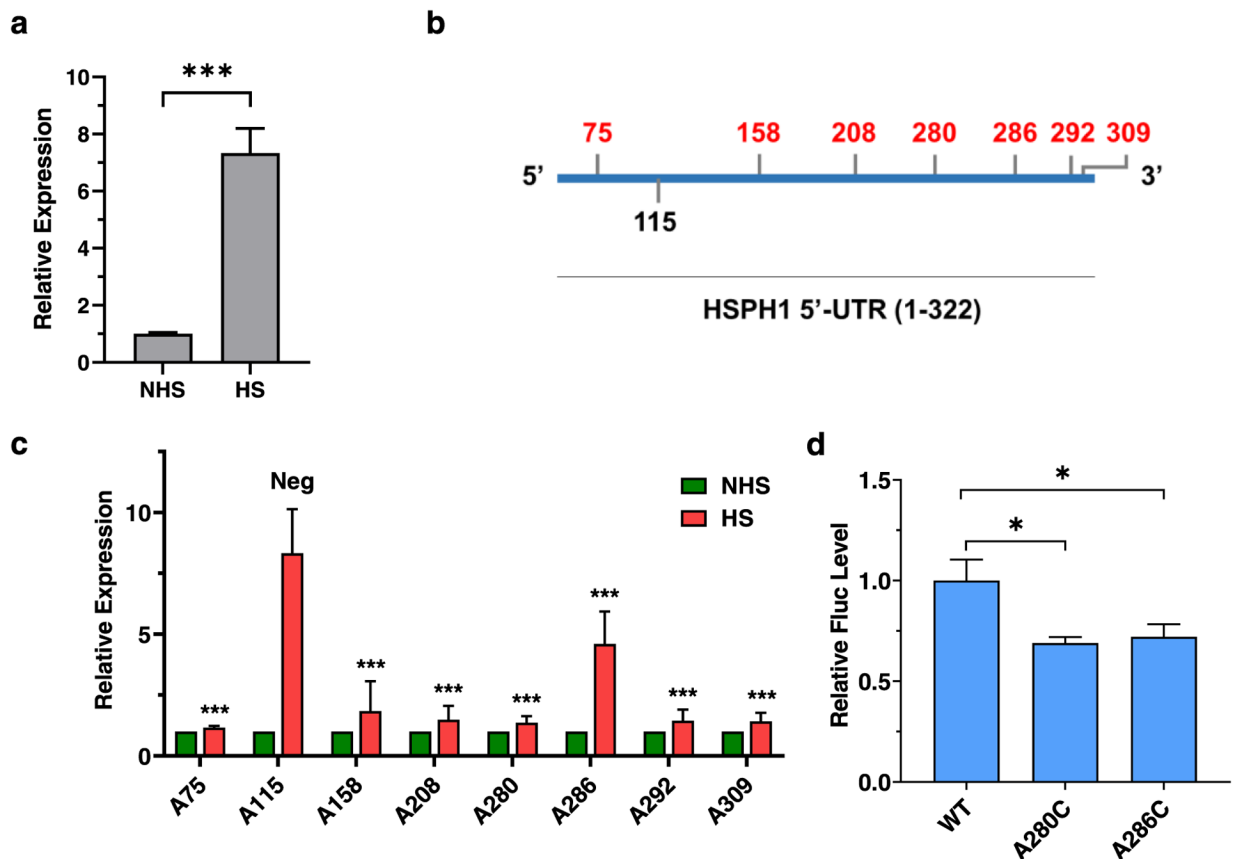
Figure 7.
Heat shock induces site-specific m^{6}A methylation to regulate the translation of *HSPH1* mRNA. (a) Real-time qPCR for the quantification of *HSPH1* transcript levels in M14 cells with (HS) or without (NHS) a 1 h heat shock treatment and recovered for 6 h. The signal of *HSPH1* transcripts was first normalized against that of *GAPDH*, and the results obtained from cells with heat shock were further normalized against that of the non-heat shock control. (b) Diagram showing the potential m^{6}A (G**A**C) (red) and the negative control (black) sites in the 5′-UTR of *HSPH1* mRNA (isoform 1) monitored by the SELECT assay. (c) SELECT assay showing the methylation level of the G**A**C and the negative control (Neg) sites in the 5′-UTR of *HSPH1* transcript. (d) M14 cells were transfected with constructs expressing firefly luciferase (Fluc) reporter with WT 5′-UTR of *HSPH1* or those with A → C mutations at the indicated m^{6}A sites. Cells were treated with heat shock and recovered for 6 h. Fluc activities were subsequently measured and normalized to that of the cotransfected Renilla luciferase. The data in (a), (c), and (d) represent the mean ± SD of results obtained from three biological replicates. The *p*-values in (a) and (d) were calculated using the two-tailed unpaired *t*-test (*, $0.01 < p < 0.05$; ***, $p < 0.001$), and the *p*-value in (c) was calculated using the ordinary two-way analysis of variance (ANOVA) (***, $p < 0.001$).